Evaluation of some charged particle induced thermonuclear reaction rates

H.R. Weller, T. TUNL Radiative Capture Group

Evaluations of Thermonuclear Proton Capture Reaction Rates for ^{2}H, ^{7}Li, ^{9}Be, and ^{11}B

S. O. Nelson[1,2], *E. A. Wulf*[1,2], *J. H. Kelley*[2,3], *and H. R. Weller*[1,2]
[1] *Department of Physics, Duke University, Durham, North Carolina, 27708*
[2] *Triangle Universities Nuclear Laboratory, Duke Station, Durham, North Carolina, 27708*
[3] *Department of Physics, North Carolina State University, Raleigh, North Carolina, 27695*

Abstract

Recent measurements and analyses of proton induced radiative-capture reactions in the vicinity of E_p=100 keV performed at the Triangle Universities Nuclear Laboratory are used to calculate the thermonuclear reaction rates of relevance in astrophysical plasmas for the reactions: D(p,γ)^{3}He, ^{7}Li(p,$\gamma_{0,1}$)^{8}Be, ^{9}Be(p,$\gamma_{0,1,2,3}$)^{10}B, and ^{11}B(p,$\gamma_{0,1}$)^{12}C. Higher energy data from previous measurements were included when possible. The Maxwellian-averaged reaction rates, obtained using numerical integration techniques, are presented in tabular form as a function of temperature. Capture to the ground and excited states are treated separately, thus allowing the determination of inverse reaction rates for specified target states. The high temperature cut-offs of the reaction rate calculations are discussed. The results are compared to those presented in the recent NACRE compilation, where appropriate, and new analytical approximations for the total reaction rates are presented in a standard form.

1. Introduction

A recent publication by the NACRE collaboration [1], presented a compilation of charged particle induced thermonuclear reaction rates. As pointed out in that paper, the absolute normalization of cross section data and the extrapolation of the data to low energies are critical to the calculated rates. The extrapolations are affected by a number of experimental and theoretical considerations. Among the important contributions of the TUNL work to *the calculation presented below are the experimentally determined values of the analyzing powers, obtained using* polarized beams. In several cases, these results help resolve ambiguities in the parameters of the reaction formalism, and thereby lead to more reliable extrapolations. Other contributions from the TUNL work are the direct measurements of cross sections at energies below E_p=100 keV. These results eliminate or reduce the amount of extrapolation necessary and should therefore provide more reliable results. In the present paper, we are presenting results for the four reactions we have studied using low energy polarized and unpolarized proton beams. As will be seen, these results are somewhat different than those presented in Ref. [1]. A discussion of the differences between the present and previous results will be presented, along with an attempt to explain the reasons for the differences. In the interest of future calculations of a(γ,x)b reaction rates, the rates for production of gamma rays from proton capture to the ground and excited states are treated separately. Because plasmas with typical astrophysical temperatures are too cool to generate significant numbers of high-energy gamma rays thermally, these reactions are expected to be significant contributors to the gamma spectrum inside stars. For consistency with the compilation, we also provide analytical approximations (good to within 5%) for the hydrogen-burning rates at the end of the paper in the form of rational polynomials.

2. Formalism and Calculations

For two-body reactions, the Maxwellian-averaged reaction rates, $N_A<\sigma v>$ are given by:

$$N_A < \sigma v >= N_A \frac{(8/\pi)^{1/2}}{\mu^{1/2}(k_B T)^{3/2}} \int_0^\infty \sigma E e^{-E/k_B T} dE \qquad (1)$$

where N_A is the Avogadro number, μ is the reduced mass of the system, k_B is the Boltzmann constant, T is the temperature, σ is the cross section at the center of mass energy (E), and v is the relative velocity of the nucleus and the proton. As in Ref. [1], all reaction rates in this paper are given in units of $cm^3 mol^{-1} s^{-1}$.

In the present work, the evaluation of this integral was performed using numerical integration techniques (Ref [2]). The method used was the one given in the operating package Mathematica. This package utilizes an adaptive Gauss-Kronrod algorithm to calculate the value of the integral to a high degree of accuracy. Regions of fast variation in the integral are automatically subdivided into smaller sub-regions and integrated separately to minimize the error in the quadrature. Peak values of narrow resonances were explicitly included in the energy range of integration so that the Mathematica package would be certain to subdivide these regions of integration as many times as necessary to minimize integration errors. The final values of the integral reported here did not change to five or more decimal places when the number of quadrature points was increased or in comparison with an evaluation using the trapezoid rule. The overall errors from the numerical integration are believed to be insignificant in comparison to the errors in the data themselves. In some cases, the data used in the evaluation of reaction rates did not extend high enough in energy to evaluate rates up to T_9=10, where T_9 is the temperature in units of 10^9 K. Typically, the upper limit of Eq 1. is taken to be $E_0 + 3\delta E$, where E_0 and δE are the peak and width of the Gamow window, the energy range in which most of the stellar burning for a reaction takes place. Expressions for E_0 and δE have been derived assuming a constant S-factor, however, and ignore its usual energy-dependent structure. In this evaluation, we have examined each integrand in order to determine the temperature range for which accurate results can be obtained. The temperature for which the energy-dependent integrand was roughly three orders of magnitude higher at its peak value than at the energy of the highest data point was considered to be the maximum T_9 that could be tabulated with certainty. As an example, a plot of the integrand of Eq. 1 for the highest value of T_9 considered for the case of $^9Be(p,\gamma)^{10}B$ is shown in Fig. 1.

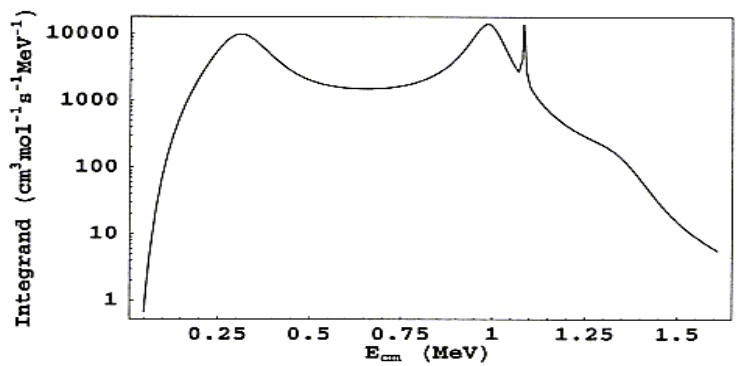

Figure 1: Integrand of Eq. (1) for $^9Be(p,\gamma)^{10}B$ at T_9=1.75 as a function of center-of-mass energy.

3. Reaction Rates

All of the tables to be presented in this paper will give the reaction rates calculated from Equation (1) for proton capture to the ground (R_{γ_0}) and excited states ($R_{\gamma_{1\to n}}$), as a function of T_9, the temperature in units of 10^9 K. All energies in the tables are in units of MeV. Finally, the ratios of the present evaluated total reaction rates (R_T) to those of the NACRE collaboration [1] (R_N) are tabulated.

A. The $^2H(p,\gamma)^3He$ Reaction

The TUNL data of Ref. [4] were included in the Evaluation of Ref. [1]. In our present evaluation, we consider only the corrected TUNL data [3] in the energy range below E_p=80 keV. In this energy range, S(E)= 0.166 eV b + 0.0071 E_{cm} eV b/keV. The resulting reaction rates are shown in Table 1 below. These rates are slightly lower than the adopted values of the compilation rates of Ref [1] for $T_9 < 0.03$. The primary reason for this is that Ref. [1] included the data of Ref. [5] and the preliminary version [4] of the TUNL data [3]. In our opinion, as discussed in Ref. [3], the data of Ref. [5] were analyzed using incorrect stopping powers and should not be included in the calculation of the reaction rates. When the correct stopping powers are used, the results of Ref. [5] and the final TUNL results [3] agree within error. Since the final TUNL results are much more accurate than those of Ref. [5] and indeed determine the slope of the S-factor empirically, we have used only this data set in our evaluation. The second reason for the difference is the fact that Ref. [1] used a polynomial of degree 3 to fit the S-factor data. This gave *a non-linear S-factor even in the region of the TUNL data [3]. Since the TUNL data and the most recent 3-body* theory [3] indicate a linear S-factor up to E_p=80 keV, we have used that in the present analysis.

The present evaluation was performed using numerical integration and assuming the linear S-factor mentioned above, as reported in [3]. The S-factor used in the higher energy region was a polynomial fit to the world data set from Ref. [1]. Because this fit was not constrained to fit the previously included low-energy data, it should more accurately fit the high energy data, and results in a 10% higher reaction rate at values of T_9 near 4. The values of T_9 for which we report rates range from 0.001 to 10. The upper limit of the reaction rate integral for all cases was taken to be E_{cm} = 10 MeV, since data were available up to this energy and this energy is well above $E_0+3\delta E$ for all temperatures listed in Table 1. The lower limit of the integrals is E=0, as in Eq. 1.

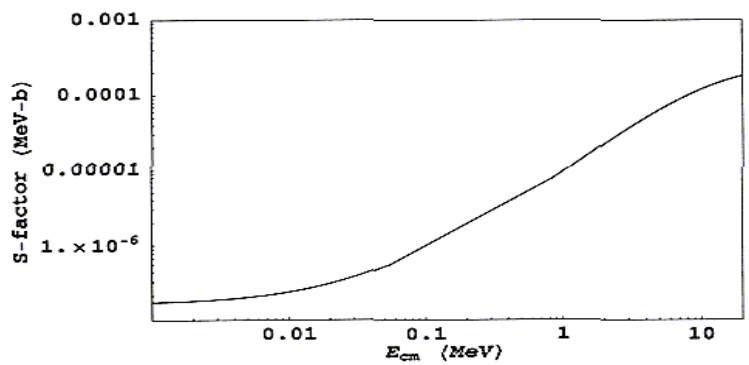

Figure 2: S-factor for $D(p,\gamma)^3He$ as a function of center-of-mass energy.

Table 1: Table of rates for the $^2H(p,\gamma)^3He$ reaction.

T_9	Rate	R_T/R_N	T_9	Rate	R_T/R_N	T_9	Rate	R_T/R_N
0.001	1.2e-11	0.923	0.04	0.4236	1.	0.5	118.6	1.02
0.002	1.649e-8	0.921	0.05	0.853	1.01	0.6	156.9	1.02
0.003	5.349e-7	0.922	0.06	1.457	1.03	0.7	197.5	1.02
0.004	4.749e-6	0.926	0.07	2.237	1.04	0.8	240.3	1.02
0.005	2.232e-5	0.926	0.08	3.189	1.04	0.9	284.8	1.03
0.006	7.242e-5	0.931	0.09	4.306	1.05	1.	331.	1.03
0.007	1.85e-4	0.934	0.1	5.576	1.05	1.25	452.2	1.04
0.008	4.003e-4	0.938	0.11	6.992	1.05	1.5	580.4	1.06
0.009	7.681e-4	0.94	0.12	8.542	1.06	1.75	713.9	1.07
0.01	1.345e-3	0.941	0.13	10.22	1.06	2.	851.7	1.07
0.011	2.195e-3	0.946	0.14	12.01	1.05	2.5	1137.	1.08
0.012	3.384e-3	0.948	0.15	13.91	1.05	3.	1431.	1.1
0.013	4.981e-3	0.951	0.16	15.9	1.05	3.5	1731.	1.1
0.014	7.059e-3	0.954	0.18	20.17	1.06	4.	2034.	1.11
0.015	9.688e-3	0.959	0.2	24.77	1.05	5.	2632.	1.11
0.016	1.294e-2	0.958	0.25	37.48	1.04	6.	3200.	1.09
0.018	2.158e-2	0.963	0.3	51.63	1.03	7.	3714.	1.06
0.02	3.353e-2	0.966	0.35	66.97	1.03	8.	4161.	1.02
0.025	8.099e-2	0.977	0.4	83.33	1.02	9.	4533.	0.983
0.03	0.1587	0.986	0.45	100.6	1.02	10.	4832.	0.936

B. The $^7Li(p,\gamma_{0,1})^8Be$ Reactions

The results reported in Ref. [1] are based on data of Ref. [6] and correspond to the sum of the reaction rates for the $^7Li(p,\gamma_0)^8Be$ and the $^7Li(p,\gamma_1)^8Be$ reactions. The TUNL contribution in this case consists of measurements of the slopes of the S-factors below E_p=100 keV for both of these channels (Ref. [7]). Direct measurements of the cross sections for these reactions were performed between E_p= 40 and 100 keV. The extracted slopes were found to be negative for both cases. As can be seen in Ref. [7], these negative slopes were attributed to previously ignored effects of the sub-threshold state at 16.6 MeV in ^8Be. In the present evaluation of the reaction rates, we have treated γ_0 and γ_1 separately. These reaction rates are presented in Table 2. We have used the TUNL results below E_p=100 keV, and the data of Ref. [6] at higher energies. Note that the evaluation of Ref [1] also uses the data of Ref. [6] (but for $\gamma_0 + \gamma_1$) but assumes that the S-factor is constant below 200 keV.

We have also adopted the absolute cross sections of Ref. [6] for the γ_0 channel. However, the ratio of γ_1 to γ_0 deduced from the results of Ref. [6] is in disagreement with that obtained by other authors (Refs. [7], [8]) in an energy range where the data overlap. The γ_0 peak is relatively narrow and easy to resolve from the rest of the data, but the γ_1 peak is 1500 keV wide and sits atop a much larger and more complex background. It is also larger than the γ_0 peak at low energies, and therefore important in calculating the total reaction rate. The data for Refs. [7] and [8] were taken with anti-coincidence shielding around the NaI detectors to remove background from beneath the γ_1 peak and better resolve the two peaks. Because of this, we have adopted a weighted average of the ratio of Ref. [6] and the new ratios from Refs. [7] and [8], and renormalized the γ_1 data of Ref. [6] to be consistent with this ratio. The resultant forms of S(E) used at low energies are S(E)=0.50 keV b - 0.00095 E_{cm} b for γ_0, and S(E)=1.52 keV b - 0.0025 E_{cm} b for γ_1.

Plots of the final S-factors as a function of energy are presented in Fig. 3 below. As in the case above, Eq. 1 was evaluated using these results in order to obtain the S-factors for both γ_0 and γ_1 which are tabulated below. In order to make a direct comparison with the results tabulated in Ref [1], the summed values are also given. The renormalization of the γ_1 cross section is one of the principle reasons for the difference of 45% between the present results and the adopted results of Ref [1], as shown in Table 2. The negative slopes below 100 keV also have an impact on the reaction rates below a T_9 of 0.006, leading to an additional increase of about 20% at the lowest value of T_9. At higher T_9 the integrand of Eq. 1 is highest in the region of the resonance, where the γ_0 S-factor is higher than the γ_1 S-factor. At these temperatures the difference between the present work and the compilation decreases

to 15%.

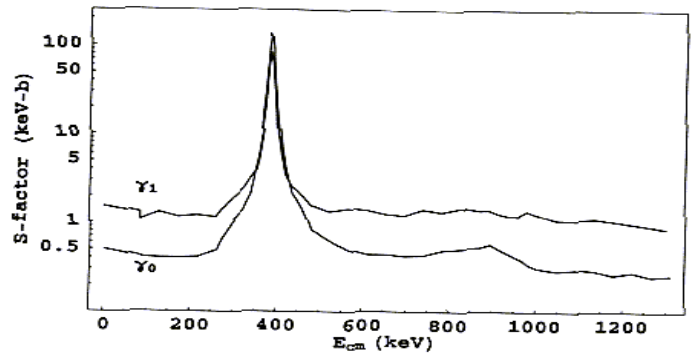

Figure 3: S-factors for $^7Li(p,\gamma_{0,1})^8Be$ as functions of center-of-mass energy.

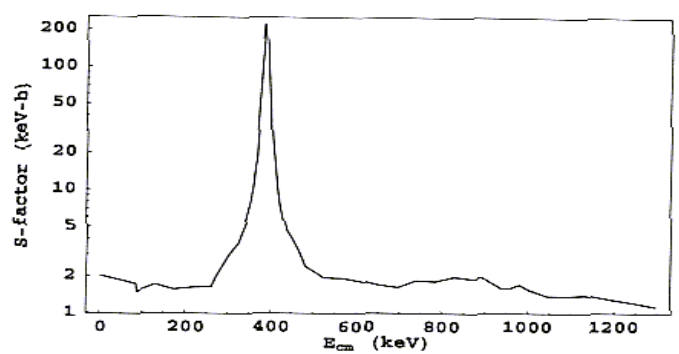

Figure 4: Total S-factor for $^7Li(p,\gamma)^8Be$ as a function of center-of-mass energy.

Table 2: Table of rates for the $^7Li(p,\gamma_{0,1})^8Be$ reactions.

T_9	$Rate_{\gamma_0}$	$Rate_{\gamma_1}$	$Rate_{\gamma_0+\gamma_1}$	R_T/R_N	T_9	$Rate_{\gamma_0}$	$Rate_{\gamma_1}$	$Rate_{\gamma_0+\gamma_1}$	R_T/R_N
0.001	1.152e-28	3.504e-28	4.656e-28	1.66	0.08	8.865e-2	0.2725	0.3611	1.46
0.002	2.712e-21	8.253e-21	1.096e-20	1.59	0.09	0.1729	0.5308	0.7037	1.45
0.003	9.969e-18	3.035e-17	4.032e-17	1.56	0.1	0.3066	0.9387	1.245	1.44
0.004	1.746e-15	5.318e-15	7.064e-15	1.54	0.11	0.5046	1.541	2.045	1.43
0.005	6.833e-14	2.081e-13	2.765e-13	1.53	0.12	0.7827	2.383	3.166	1.43
0.006	1.114e-12	3.395e-12	4.51e-12	1.52	0.13	1.157	3.513	4.671	1.42
0.007	1.032e-11	3.145e-11	4.177e-11	1.51	0.14	1.645	4.981	6.626	1.41
0.008	6.455e-11	1.968e-10	2.613e-10	1.5	0.15	2.262	6.836	9.097	1.4
0.009	3.033e-10	9.248e-10	1.228e-9	1.5	0.16	3.024	9.124	12.15	1.39
0.01	1.148e-9	3.5e-9	4.648e-9	1.49	0.18	5.048	15.2	20.24	1.37
0.011	3.669e-9	1.119e-8	1.486e-8	1.49	0.2	7.839	23.56	31.39	1.35
0.012	1.025e-8	3.127e-8	4.152e-8	1.49	0.25	19.07	56.64	75.71	1.32
0.013	2.566e-8	7.829e-8	1.039e-7	1.48	0.3	39.67	111.6	151.3	1.3
0.014	5.864e-8	1.79e-7	2.376e-7	1.48	0.35	80.63	197.5	278.1	1.28
0.015	1.242e-7	3.79e-7	5.032e-7	1.48	0.4	166.8	331.1	497.9	1.25
0.016	2.464e-7	7.522e-7	9.986e-7	1.48	0.45	337.4	537.6	874.9	1.22
0.018	8.267e-7	2.525e-6	3.352e-6	1.48	0.5	639.	845.6	1485.	1.2
0.02	2.34e-6	7.151e-6	9.492e-6	1.47	0.6	1800.	1866.	3665.	1.17
0.025	1.87e-5	5.718e-5	7.588e-5	1.46	0.7	3848.	3506.	7353.	1.16
0.03	9.058e-5	2.772e-4	3.678e-4	1.46	0.8	6756.	5740.	1.25e4	1.16
0.04	8.906e-4	2.731e-3	3.621e-3	1.46	0.9	1.034e4	8446.	1.879e4	1.15
0.05	4.471e-3	1.373e-2	1.82e-2	1.46	1.	1.436e4	1.147e4	2.583e4	1.15
0.06	1.518e-2	4.666e-2	6.183e-2	1.46	1.25	2.491e4	1.949e4	4.441e4	1.15
0.07	4.003e-2	0.1231	0.1631	1.46	1.5	3.445e4	2.706e4	6.151e4	1.15

C. The $^9Be(p,\gamma_{0,1,2,3})^{10}B$ Reactions

The TUNL contribution in this case consists of high- resolution measurements which allowed for a direct separation of the four final states, and polarized beam measurements at E_p= 100 and 280 keV, which fixed several ambiguous parameters and led to more reliable direct-capture-plus-resonances calculations for capture to the four separate final states.(Refs. [9], [10]) Polarized beam measurements were used to establish the fact that the 7.542 MeV state in ^{10}B had a spin and parity of 2^+, not 2^- as assumed in the analysis Ref. [11]. While this new assignment causes the total reaction rate to differ from that of Ref. [1] by only as much as 10%, it has a larger impact on the extrapolation for the case of capture to the ground state of ^{10}B. As shown in Ref. [10], the value of S(0) for the reaction leading to the ground state is about 40% lower when a 2^+ assignment is adopted. This reduction in S-factor for capture to the ground state, when combined with the S-factors for capture to the first three excited states, gives a total S-factor of S(0)=0.93 keV b, lower than S(0)=1 keV b proposed by Ref. [11]. The four S-factors plotted below in Fig. 5, taken from Refs. [9] and [10], are the basis for the present analysis. The reaction rates given below (Table 3) for each of the four final states were obtained by numerically integrating these curves.

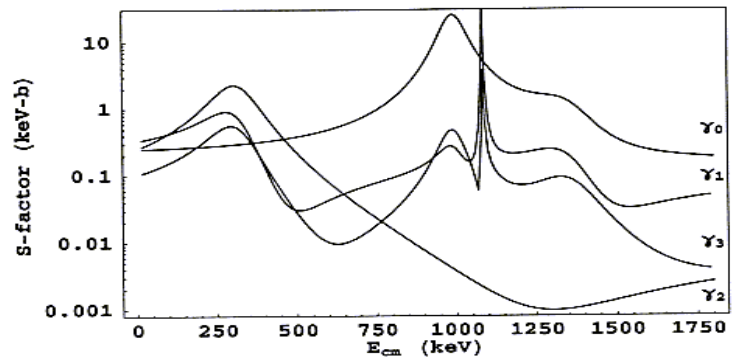

Figure 5: S-factors for $^9Be(p,\gamma_{0,1,2,3})^{10}B$ as functions of center-of-mass energy.

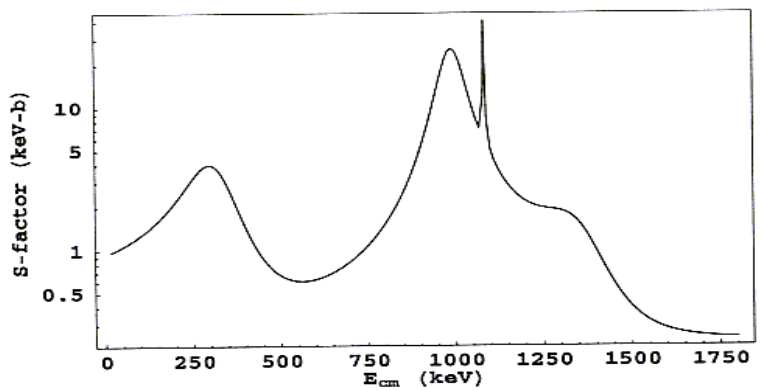

Figure 6: Total S-factor for $^9Be(p,\gamma)^{10}B$ as a function of center-of-mass energy.

Table 3: Table of rates for the $^{9}Be(p,\gamma_{0,1,2,3})^{10}B$ reactions.

T_9	$Rate_{\gamma_0}$	$Rate_{\gamma_1}$	$Rate_{\gamma_2}$	$Rate_{\gamma_3}$	$Rate_{\gamma_0+\gamma_1+\gamma_2+\gamma_3}$	R_T/R_N
0.003	1.167e-23	1.572e-23	1.217e-23	4.917e-24	4.448e-23	1.1
0.004	6.767e-21	9.141e-21	7.098e-21	2.864e-21	2.587e-20	1.08
0.005	6.213e-19	8.413e-19	6.555e-19	2.641e-19	2.382e-18	1.07
0.006	1.945e-17	2.639e-17	2.063e-17	8.299e-18	7.476e-17	1.06
0.007	3.033e-16	4.125e-16	3.234e-16	1.299e-16	1.169e-15	1.04
0.008	2.919e-15	3.977e-15	3.127e-15	1.255e-15	1.128e-14	1.03
0.009	1.975e-14	2.696e-14	2.126e-14	8.519e-15	7.649e-14	1.03
0.01	1.024e-13	1.4e-13	1.107e-13	4.43e-14	3.973e-13	1.03
0.011	4.309e-13	5.904e-13	4.679e-13	1.871e-13	1.676e-12	1.02
0.012	1.536e-12	2.109e-12	1.675e-12	6.691e-13	5.989e-12	1.02
0.013	4.784e-12	6.578e-12	5.238e-12	2.09e-12	1.869e-11	1.01
0.014	1.332e-11	1.834e-11	1.464e-11	5.835e-12	5.213e-11	1.01
0.015	3.374e-11	4.655e-11	3.724e-11	1.483e-11	1.324e-10	1.
0.016	7.891e-11	1.09e-10	8.741e-11	3.477e-11	3.101e-10	1.
0.018	3.543e-10	4.911e-10	3.954e-10	1.57e-10	1.398e-9	0.991
0.02	1.289e-9	1.793e-9	1.45e-9	5.746e-10	5.107e-9	0.988
0.025	1.707e-8	2.391e-8	1.954e-8	7.707e-9	6.823e-8	0.976
0.03	1.218e-7	1.718e-7	1.417e-7	5.568e-8	4.91e-7	0.967
0.04	2.114e-6	3.023e-6	2.54e-6	9.898e-7	8.667e-6	0.951
0.05	1.595e-5	2.312e-5	1.978e-5	7.646e-6	6.65e-5	0.943
0.06	7.412e-5	1.088e-4	9.471e-5	3.634e-5	3.14e-4	0.94
0.07	2.517e-4	3.745e-4	3.314e-4	1.262e-4	1.084e-3	0.942
0.08	6.883e-4	1.037e-3	9.331e-4	3.528e-4	3.011e-3	0.947
0.09	1.607e-3	2.453e-3	2.244e-3	8.421e-4	7.145e-3	0.953
0.1	3.329e-3	5.148e-3	4.789e-3	1.784e-3	1.505e-2	0.959
0.11	6.286e-3	9.849e-3	9.314e-3	3.445e-3	2.889e-2	0.966
0.12	1.102e-2	1.75e-2	1.683e-2	6.178e-3	5.152e-2	0.97
0.13	1.818e-2	2.927e-2	2.863e-2	1.043e-2	8.651e-2	0.974
0.14	2.854e-2	4.658e-2	4.635e-2	1.677e-2	0.1382	0.98
0.15	4.297e-2	7.111e-2	7.201e-2	2.585e-2	0.2119	0.981
0.16	6.243e-2	0.1048	0.108	3.847e-2	0.3137	0.98
0.18	0.1207	0.2086	0.2231	7.819e-2	0.6306	0.982
0.2	0.2127	0.3787	0.4208	0.145	1.157	0.981
0.25	0.6587	1.263	1.552	0.512	3.986	0.977
0.3	1.554	3.187	4.331	1.368	10.44	0.976
0.35	3.078	6.641	9.911	3.007	22.64	0.98
0.4	5.403	12.03	19.49	5.712	42.63	0.991
0.45	8.694	19.55	34.04	9.683	71.97	1.01
0.5	13.1	29.24	54.11	15.01	111.5	1.02
0.6	25.91	54.34	110.9	29.54	220.7	1.05
0.7	45.31	84.95	186.8	48.23	365.3	1.06
0.8	73.94	118.4	275.6	69.47	537.4	1.07
0.9	116.7	152.7	371.1	91.82	732.3	1.05
1.	181.5	186.7	467.7	114.3	950.2	1.03
1.25	514.	270.2	692.	168.	1644.	0.967
1.5	1236.	362.	871.5	219.4	2689.	0.921
1.75	2460.	477.9	1003.	273.	4214.	0.914

D. The $^{11}B(p,\gamma_{0,1})^{12}C$ Reactions

The data set used in our evaluation differed from that used in the evaluaton of Ref. [1] in several respects. First of all, the extrapolation to very low energies was taken from the TUNL work [12], which used polarized and unpolarized capture data in the E_p = 80-100 keV range and a direct-capture-plus-resonances model to perform this extrapolation. Second, the strength of the E_{cm}=149 keV resonance was taken from the recent work of Cecil et al. [13]. And finally, the only higher energy data which were used in the present work were those of Allas and Segel et al. [14],[15]. A plot of the final S-factor data used in the present evaluation is shown in Fig. 8 below. Note that this plot represents the sum of the capture strengths leading to the ground and first excited states of ^{12}C. The extrapolated value of S(0) for capture to both states is 5.28 keV b, nearly 60% higher than that adopted by the NACRE compilation. Rates for capture to the ground and first excited states are shown separately in Table 4. The present rates for capture to both the ground and first excited states (Table 4) are a factor of 2 greater than those in Ref. [1] from T_9=0.004 up to T_9=0.02. This is a result of the new TUNL extrapolation by (Ref. [12]). This ratio rises to 2.7 for T_9 in the range of 0.02-0.07, due to the new TUNL extrapolation and the use of the strength for the 149 keV resonance obtained from the more recent work by Cecil, et al. [13]. In this range, the interference between the direct and resonance capture has a large effect. The present rates rapidly approach those in Ref. [1] as the temperature increases and the integral covers the total area of the resonance. A slight (15%) disagreement re-appears when the integrand is larger in the high-energy tail region of the resonance (the location of the peak of the Gamow window), again due to the different resonance parameters used. This disagreement disappears at higher values of T_9 as the dominant contribution to the integral comes from the higher-energy data.

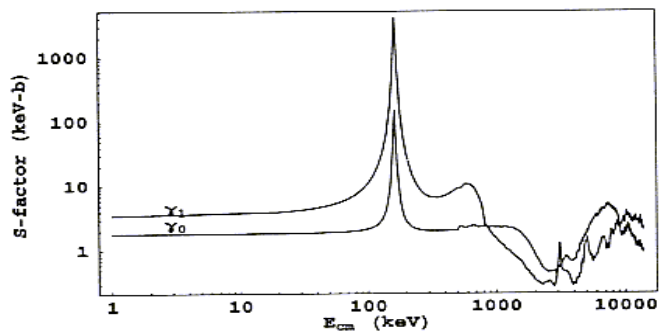

Figure 7: S-factors for $^{11}B(p,\gamma_{0,1})^{12}C$ as functions of center-of-mass energy.

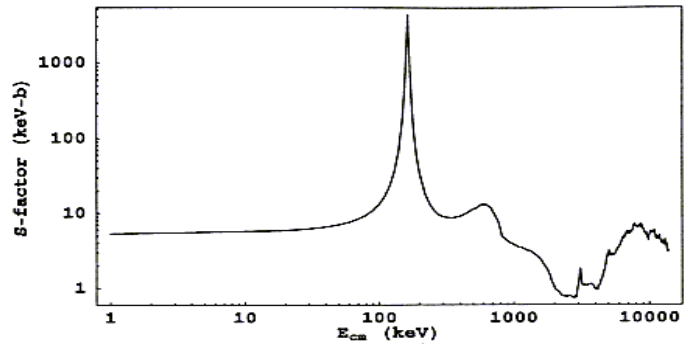

Figure 8: Total S-factor for $^{11}B(p,\gamma)^{12}C$ as a function of center-of-mass energy.

Table 4: Table of rates for the $^{11}B(p,\gamma_{0,1})^{12}C$ reaction.

T_9	$Rate_{\gamma_0}$	$Rate_{\gamma_1}$	$Rate_{\gamma_0+\gamma_1}$	R_T/R_N	T_9	$Rate_{\gamma_0}$	$Rate_{\gamma_1}$	$Rate_{\gamma_0+\gamma_1}$	R_T/R_N
0.004	9.701e-25	1.973e-24	2.943e-24	2.03	0.15	5.487e-2	1.124	1.179	1.06
0.005	1.95e-22	4.001e-22	5.951e-22	2.04	0.16	9.721e-2	2.067	2.164	1.05
0.006	1.11e-20	2.297e-20	3.407e-20	2.12	0.18	0.2546	5.663	5.918	1.03
0.007	2.795e-19	5.826e-19	8.621e-19	2.01	0.2	0.5512	12.56	13.11	1.02
0.008	3.993e-18	8.386e-18	1.238e-17	1.99	0.25	2.188	50.73	52.92	1.01
0.009	3.775e-17	7.985e-17	1.176e-16	2.	0.3	5.393	123.6	129.	1.01
0.01	2.611e-16	5.561e-16	8.171e-16	2.01	0.35	10.18	226.8	236.9	1.02
0.011	1.414e-15	3.034e-15	4.448e-15	2.01	0.4	16.37	350.1	366.4	1.03
0.012	6.306e-15	1.362e-14	1.992e-14	2.01	0.45	23.83	483.3	507.2	1.04
0.013	2.398e-14	5.215e-14	7.613e-14	2.02	0.5	32.49	619.	651.5	1.05
0.014	7.996e-14	1.751e-13	2.55e-13	2.02	0.6	53.69	881.8	935.5	1.08
0.015	2.387e-13	5.262e-13	7.649e-13	2.03	0.7	81.17	1127.	1208.	1.11
0.016	6.487e-13	1.44e-12	2.088e-12	2.03	0.8	116.6	1360.	1476.	1.13
0.018	3.8e-12	8.547e-12	1.235e-11	2.05	0.9	161.5	1591.	1753.	1.15
0.02	1.74e-11	3.966e-11	5.706e-11	2.07	1.	217.1	1829.	2046.	1.16
0.03	3.707e-9	9.046e-9	1.275e-8	2.15	1.25	408.4	2471.	2880.	1.17
0.04	1.079e-7	2.832e-7	3.911e-7	2.27	1.5	677.	3174.	3851.	1.16
0.05	1.181e-6	3.365e-6	4.546e-6	2.42	1.75	1019.	3893.	4912.	1.14
0.06	7.328e-6	2.312e-5	3.045e-5	2.6	2.	1424.	4589.	6014.	1.12
0.07	3.181e-5	1.178e-4	1.497e-4	2.71	3	3425.	6789.	1.021e4	1.08
0.08	1.104e-4	5.409e-4	6.514e-4	2.39	4	5520.	8071.	1.359e4	1.06
0.09	3.372e-4	2.401e-3	2.738e-3	1.86	5	7367.	8788.	1.615e4	1.05
0.1	9.55e-4	9.702e-3	1.066e-2	1.5	6	8943.	9237.	1.818e4	1.04
0.11	2.531e-3	3.363e-2	3.616e-2	1.3	7	1.036e4	9581.	1.994e4	1.03
0.12	6.207e-3	9.892e-2	0.1051	1.2	8	1.177e4	9921.	2.169e4	1.02
0.13	1.397e-2	0.2508	0.2647	1.13	9	1.329e4	1.032e4	2.361e4	1.02
0.14	2.882e-2	0.5599	0.5887	1.09	10	1.503e4	1.079e4	2.582e4	1.02

E. Analytical Approximations (5%):

The last table in each section gives the total hydrogen-burning rate for that section's $X(p,\gamma_{0+...+n})Y$ reactions as a function of T_9, in units of $cm^3mol^{-1}s^{-1}$. These rates are given (in the same units as in the tables) to within 5% by $Rate=10^{(P_1/P_2)}$, where P_1/P_2 is a rational polynomial fit to the calculated rates. P_1 and P_2 are simple polynomials of the form $C_0 + C_1x + C_2x^2+...$, and x is given by $\log_{10}(T_9)$. The polynomials were kept to the minimum number of terms necessary to achieve 5% agreement with the calculation. Table 5 gives the coefficients of P_1 in line 1 and P_2 in line 2 for each set of reactions investigated. The ranges of T_9 for which these fits are valid are listed, and are the same as the ranges of T_9 covered by the tables.

$^2H(p,\gamma)^3He$ $(0.001 \leq T_9 \leq 10)$

C_0	C_1	C_2	C_3	C_4
2.5219	-0.27769	-0.45442	1.0250	
1.0000	-0.66315	0.25810	0.15150	0.016891

$^7Li(p,\gamma_{0+1})^8Be$ $(0.001 \leq T_9 \leq 1.5)$

C_0	C_1	C_2	C_3	C_4	C_5	C_6	C_7
4.4036	17.908	32.769	18.820	-3.8774	-5.0843	-1.8262	-0.31777
1.0000	3.4326	6.1788	2.6802	0.45811	0.048868		

$^9Be(p,\gamma_{0+1+2+3})^{10}B$ $(0.003 \leq T_9 \leq 1.75)$

C_0	C_1	C_2	C_3	C_4	C_5	C_6
2.9584	16.839	62.184	73.54	15.299	0.6178	1.4941
1.0000	4.8577	16.283	8.3569	0.9027		

$^{11}B(p,\gamma_{0+1})^{12}C$ $(0.004 \leq T_9 \leq 10)$

C_0	C_1	C_2	C_3	C_4	C_5	C_6	C_7	C_8	C_9
3.3125	7.7747	9.5934	0.952166	-18.977	-15.417	7.9898	9.4787	-1.3104	-1.4212
1.0000	1.8951	1.9525	-0.93618	-3.9983	-1.6813	1.4583	0.76681	0.00587	-0.015047

Table 5. Coefficients for $X(p,\gamma)Y$ reaction rate polynomials.

This work was supported in part by USDOE grants No. DE-FG02-97ER41033, DE-FG02-97ER41042, and DE-FG02-9741046.

References

[1] C. Angulo, et al., Nuc. Phys. **A349**, (1990), 210.

[2] S. Wolfram, The Mathematica Book (Cambridge University Press, 1996).

[3] G. Schmid *et al.*, Phys. Rev. **C56**, (1997), 2565.

[4] G. Schmid, Ph. D. thesis, Duke University, 1995.

[5] G.M. Griffiths, M. Lal,C.D. Scarfe, Can. Journ. Phys. **41**, (1963), 724.

[6] D. Zahnow *et al.*, Z. Phys. **A351**, (1995), 229.

[7] M. Spraker, *et al.*, Phys. Rev. **C61**, (1999), 015802/1.

[8] M.A. Godwin *et al.*, Phys. Rev. **C56**, (1997), 1605.

[9] E.A. Wulf *et al.*, Phys. Rev. **C58**, (1998), 517.

[10] S.J. Gaff *et al.*, Phys. Rev. **C59**, (1999), 3425.

[11] D. Zahnow *et al.*, Nuc. Phys. **A589**, (1995), 95.

[12] J.H. Kelley *et al.*, to be published in Phys. Rev. C.

[13] F.E. Cecil *et al.*, Nuc. Phys. **A539**, (1992), 75.

[14] R.E. Segel, S.S. Hanna, and G. Allas, Phys. Rev. **B139**, (1965), 818.

[15] R.G. Allas, S.S. Hanna, L. Meyer-Schutzmeister, and R.E. Segel, Nuc. Phys. **A58**, (1964), 122.